Structural Characteristics of Eucalyptus Lignin Regulated through Alkali Cooking Process

Zheng Shen,[a,b] Yi Liu,[a,b] Xiaoxiao Wei,[a,b] Liming Zhang,[a,b] Ling Zeng,[c] Shuangfei Wang,[a,b,d] and Douyong Min [a,b,*]

Understanding the basic chemical structure of lignin macromolecules can facilitate the development of lignin-based materials. In this study, the lignin structure was regulated through different alkali cooking conditions. The acid precipitated lignin from the spent cooking liquor was purified and fractionated with different organic solvents. The lignin samples with different structures were obtained by regulating the cooking time. The structural characteristics of the lignin preparations were systematically investigated. The results revealed that the structure of lignin was regulated by the heating time and the residence time during the cooking process. Non-condensed lignin was achieved after a specific cooking condition; it had higher molecular weight (9686 g/mol), more β-O-4 linkages (25.3/100Ar), but lower phenolic hydroxyl content (1.51 mmol/g) than the counterpart pulping with longer time duration. The non-condensed lignin also had excellent thermal stability. Compared with industrial lignin, the lignin with non-condensed structure can be modified to obtain phenolic resin materials with better performance. The non-condensed structure with the specific characteristics can broaden the valorization of lignin for producing biochemical and biomaterials.

DOI: 10.15376/biores.17.3.4226-4240

Keywords: Lignin; Structural characteristics; Cooking; Regulation

*Contact information: a: College of Light Industry and Food Engineering, Guangxi University, Nanning 530004, PR China; b: Guangxi Key Laboratory of Clean Pulp & Papermaking and Pollution Control, Nanning 530004, PR China; c: Nanning Ketian Waterborne Technologies Co., Ltd., Nanning 530105, PR China; d: Guangxi Bossco Environmental Protection Technology Co., Ltd, Nanning 530007, PR China; * Corresponding author: mindouyong@gxu.edu.cn*

INTRODUCTION

Lignin exists mainly in woody and herbaceous plants, and also in all other vascular plants. In nature, its abundance is second only to cellulose and chitin, and it is the third most abundant natural macromolecular organic substance. Lignin contains macromolecular polyphenols with a three-dimensional molecular structure formed through connecting the phenylpropane structural units with ether bonds and carbon-carbon bonds (Ragauskas *et al*. 2014; Lourenco *et al*. 2016). It is mainly composed of three units: syringyl (S) containing two methoxy groups, guaiacyl (G) unit containing one methoxy group, and p-hydroxyphenyl (H) unit without a methoxy group (Lourenco *et al*. 2016). The main bonds between these units are the aryl ether bonds (β-O-4, α-O-4, *etc*.) and the carbon-carbon (β-5, β-β, *etc*.) bonds (Holtman *et al*. 2007; Ragauskas *et al*. 2014). Lignin has a rich aromatic chemical structure, which makes lignin a potential resource for the manufacture of carbon fibers, aromatic compounds, phenolic resins, bio-oils, and other

polymeric materials (Gillet *et al*. 2017; Gall *et al*. 2017; Culebras *et al*. 2018; Collins *et al*. 2019).

Despite its many positive features, the industrial application of lignin is a huge challenge, due to the complexity and heterogeneity of its structure and composition, as well as its uneven distribution. The global pulp industry produces about 78 million tons of lignin every year, of which only 2% of the lignin is used to produce lignin derivatives, and the remaining 98% is burned for power generation or placed in landfills, causing pollution to the environment (Lora and Glasser 2002; Jardim *et al*. 2020; Magdeldin and Jarvinen 2020; Culebras *et al*. 2021). To better understand the inherent structure and specific properties of lignin, basic research on lignin structure and the relationship between its structure and their material properties is needed to promote its valorization (Menon and Rao 2012; Gall *et al*. 2018).

Eucalyptus is a fast-growing wood species, and it is one of the most important industrial raw materials for making pulps and fiberboards. The eucalyptus plantations in China encompass an area of 4.6 Mhm^2, and most of the harvested materials are used in the pulp and paper industry (Himmel *et al*. 2007). The black liquor produced in the pulping process contains a large amount of organic pollutants and toxic substances, but also a considerable amount of lignin. However, the current pollutants in black liquor account for more than 90% of the pollutants in the whole plant, and the discharge of black liquor is the main source of paper-making pollution.

Xiong *et al*. (2017) used the alkali lignin as raw materials co-precipitating with sodium metasilicate to prepare lignin/silica hybrid materials. Cha *et al*. (2020) proposed a new technology for direct extraction of the alkali lignin microspheres based on pH control and hydrothermal treatment. The lignin microspheres extracted from black liquor can be used in agricultural drug delivery and heavy metal removal in wastewater. Fu *et al*. (2013) used the lignin as the precursor with the steam physical activation to prepare activated carbon, which proved the practical value of its lignin-based adsorbent. Narapakdeesakul *et al*. (2013) recovered lignin from oil palm empty fruit bunch black liquor and studied the potential use of the recovered lignin in the production of liner board coatings. To study the structure of lignin, Wang *et al.* (2017) isolated MWL, CEL, and EHL preparations from different eucalyptus woods, and also prepared a modified enzyme lignin DEL based on double ball milling and enzymatic hydrolysis. The structural characteristics of lignin were studied by HPAEC, GPC, and NMR techniques. Xiao *et al*. (2019) compared the structural characteristics of lignin isolated from the heartwood, sapwood, and bark of *Eucalyptus grandis*. Chen *et al*. (2018) used CRM and NMR to describe the chemical and structural changes of eucalyptus lignin during growth.

In the present study, *Eucalyptus urophylla* wood chips were treated with different cooking severities to regulate the structural characteristics of lignin. The dissolved lignins were extracted from the spent cooking liquor, fractionated, and purified. The lignin preparations were characterized by ^{1}H-^{13}C heteronuclear single quantum coherence nuclear magnetic resonance (^{1}H-^{13}C HSQC NMR), ^{31}P nuclear magnetic resonance (^{31}P NMR), and gel permeation chromatography (GPC) (Lin *et al*. 1992; Gellerstedt *et al*. 2000; Gellerstedt *et al*. 2001; Zhang and Gellerstedt 2001; Rencoret *et al*. 2009; Kim and Ralph 2010; Zhang and Gellerstedt 2011; Meng *et al*. 2019). The results revealed that the lignin was successfully regulated *via* different cooking severities. A better understanding of the lignin structure varied with the different cooking severities can provide a theoretical basis for the value-added utilization of lignin.

EXPERIMENTAL

Materials

Eucalyptus urophylla wood chips were provided by a local pulp mill in Guangxi. The wood chips were sealed in a plastic bag to balance the moisture for the moisture measurement. Dimethyl sulfoxide-d_6, chloroform-d, and 2-chloro-4,4,5,5-tetramethyl-1,3,2-dioxaphospholane (TMDP) were purchased from Sigma-Aldrich (St. Louis, MO, USA). The analytical grade reagents, *e.g.*, sulfuric acid, acetone, acetic anhydride, pyridine, ethanol, and sodium hydroxide were purchased from Tianjin Zhiyuan Chemical Reagent Co., Ltd (Tianjin, China).

Preparation of Lignin

The cooking of wood was completed as follows. The cooking temperature was 160 °C, the amount of alkali was 20%, and the solid to liquid ratio was 1:5. The heating time (40, 50, 60, and 70 min) and the residence time (30, 60, 90, 120 min) of cooking were applied to regulate the lignin structure. The black liquor was collected and filtered after the cooking was completed. The black liquor was diluted 10 times with distilled water and then precipitated in an acidic aqueous solution (pH 2). After centrifugation, the precipitate was freeze-dried to achieve the preliminary crude lignin. The crude lignin was purified and fractionated by the different solvents. The purification steps were as follows. First, the crude lignin was suspended in acetone (1:100, g/mL). The supernatant was collected by centrifugation and freeze-dried to obtain C-X-A (X: group number, A: acetone). The precipitate was air dried and dissolved with the mixture of acetone/water (9:1, v/v). The supernatant was collected after centrifugation and freeze-dried to obtain C-X-W (X: group number, W: water/acetone). As a result, 14 lignin preparations were obtained (Table 1).

Table 1. Cooking Conditions and the Lignin Preparations

Number	Residence Time	Heating Time	Sample
C-1	30	40	C-1-A*
			C-1-W
C-2	30	50	C-2-A
			C-2-W
C-3	30	60	C-3-A*
			C-3-W
C-4	30	70	C-4-A*
			C-4-W
C-5	60	60	C-5-A
			C-5-W
C-6	90	60	C-6-A
			C-6-W
C-7	120	60	C-7-A*
			C-7-W

* Lignin samples in low molecular weight were selected for characterization

Acetylation of Lignin

The acetylation of lignin was completed as follows. First, 10 mg of lignin preparation was completely dissolved in 1 mL of pyridine, and then 1 mL of acetic anhydride was added. The reaction was completed for 24 h with continual shaking at room temperature in the dark. Next, 2 to 3 mL of ethanol was applied to terminate the reaction

in 10 min. The excessive pyridine was removed by rotary evaporation. This process was repeated several times until there was no pyridine. After freeze-drying, the acetylated lignin samples were obtained for the molecular weight analysis.

Lignin Characterization

Molecular weight analysis

The molecular weights of the acetylated lignin samples were measured by a gel permeation chromatography (GPC, Agilent 1260, Santa Clara, CA, USA) with a PLgel 15 μm MIXED-E column (Agilent) (Wen *et al*. 2013; Gong *et al*. 2016). The acetylated lignin was dissolved in THF, and its concentration was 2 mg/mL. The flow rate was 0.7 mL/min, and the column temperature was 30 °C. The injection volume was 20 μL. Polystyrene standards with different molecular weights (M_p = 580, 1920, 4750, 9570, and 27,810) were used to determine the standard curve.

^{1}H-^{13}C HSQC NMR analysis

The 2D-HSQC NMR analysis was conducted on a Bruker 500 MHz spectrometer (Karlsruhe, Germany) at 25 °C. Briefly, 80 mg of the lignin sample was dissolved with 700 μL of DMSO-d_6 in 5 mL ampoule bottles. The solution was transferred into NMR tubes. The parameters were as follows: the pulse sequence was HSQCETGPSI512, 2 K data points in the time domain, number of scans NS = 64, acquisition time AQ = 0.18 s, the spectral width of F1 = 11.49 ppm (1H), F2 = 120 ppm (13C), delay time D1 = 0.98 s, the transmitter frequency offset (O1P) = 3.2 ppm, frequency offset of 2nd nucleus (O2P) = 100 ppm. The chemical shift was corrected according to the DMSO contour (δC/δH 39.5/2.5 ppm).

^{31}P NMR analysis

The internal standard solution was prepared according to the reported method (Milotskyi *et al*. 2019). A total of 4 mmol chromium acetylacetone (the relaxation agent) was dissolved in 50 mL of pyridine followed with addition of 5 mmol N-hydroxy succinimide (the internal standard compound). Next, 15 mg of the lignin sample was dissolved with 400 μL of $CDCl_3$ in 5 mL ampoule bottles. Then, 80 μL of phosphating reagent (2-chloro-4,4,5,5-tetramethyl-1,3,2-dioxacyclopentane, TMDP) and 200 μL of the internal standard solution were added to the bottles. The mixture was quickly transferred into NMR tubes for the quantitation of phenolic hydroxyl groups as the reaction was completed in 5 min.

The ^{31}P NMR analysis was conducted on a Bruker 500 MHz spectrometer at 25 °C. The parameters were as follows: the pulse sequence was PROF19DEC, 64 K data points in the time domain, spectral width SW = 100 ppm, the center frequency O1P = 145 ppm, number of scans NS = 64, delay time D1 = 6.4 s.

Thermogravimetric analysis (TGA)

The thermal stability of the lignin samples was determined using an STA 449 F5 thermogravimetric apparatus (Netzsch, Selb, Germany). Approximately 5 to 10 mg of the sample was weighed in an Al_2O_3 crucible, placed on a balance in a furnace. It was heated at a rate of 10 °C/min under high-purity nitrogen atmosphere at a flow rate of 50 mL/min with the temperature range from 30 to 800 °C.

RESULTS AND DISCUSSION

Molecular Weight Analysis

The molecular weight of lignin is closely related to the separation and purification method (Tolbert *et al*. 2014). The number average (M_n), weight average (M_w) molecular weights, and polydispersity index (PDI, M_w/M_n) of the acetylated lignin were determined by gel permeation chromatography (GPC). As shown in Table 2, the solubility of lignin was related to its molecular weight. Therefore, the C-X-A samples of lower weight average molecular weights were obtained from supernatant. For instance, the M_w of C-1-A, C-3-A, C-4-A and C-7-A were 2192, 2583, 2716, and 2048 g/mol. The precipitate bearing higher molecular weight lignin was purified and fractionated again to obtain the C-X-W samples. The M_w of C-X-W samples showed a trend of first increasing and then decreasing with the increase of cooking severity. For instance, the M_w of C-1-W, C-2-W, C-3-W, C-4-W, C-5-W, C-6-W, and C-7-W were 8555, 7541, 9686, 9310, 9979, 8635, and 8812 g/mol, respectively. Maintaining the constant residence time (30 min), the M_w of lignin samples showed an increasing trend as the heating time increased within a certain range (40 to 70 min). The shorter heating time resulted in more lignin with lower molecular weight being dissolved at the beginning of cooking, which distributed outside of the cell wall. Maintaining the heating time (60 min) constant, the M_w of lignin samples decreased with the increase of residence time. This is because the longer residence time resulted in more cleavage of lignin, which caused a decrease in the molecular weight. Although the lignin fragments could be condensed to form new macromolecules in the black liquor, the molecular weight was still lower than C-5-W. The C-X-A samples with lower PDI were due to the more uniform dispersion of small molecules in acetone solution.

Table 2. Molecular Weight and Polydispersity (M_w/M_n) of Lignin Fractions

Sample	M_w	M_n	M_w/M_n	Yield of lignin (%)
C-1-W	8555	5209	1.64	6.29
C-2-W	7541	4870	1.55	9.83
C-3-W	9686	5546	1.75	11.11
C-4-W	9310	5527	1.68	11.27
C-5-W	9979	5747	1.74	13.21
C-6-W	8635	5286	1.63	13.86
C-7-W	8812	5127	1.72	14.33
C-1-A	2192	1873	1.17	22.53
C-3-A	2583	2168	1.19	23.60
C-4-A	2716	2203	1.23	21.88
C-7-A	2048	1777	1.15	23.90

^{1}H-^{13}C HSQC NMR analysis

^{1}H-^{13}C HSQC NMR was used to reveal the structural characteristics of lignin. The 2D HSQC NMR spectra of the lignin samples are revealed in Fig. 1. The main substructures of lignin that were identified by 2D HSQC NMR are shown in Fig. 2. The spectrum of lignin mainly contains the oxidized aliphatic region (δC/δH 50-95 / 2.5-6.0 ppm) and the aromatic region (δC/δH 95-150 / 5.5-8.0) (Kim and Ralph 2010; Chen *et al*. 2017). The linkages were identified in the side chain region, and the syringyl (S) and guaiacyl (G) units were clearly distinguished in the aromatic region (Rencoret *et al*. 2011; Wen *et al*. 2015; Wang *et al*. 2017). The main contours were assigned according to the literature (Martínez *et al*. 2008; Rencoret *et al*. 2009; Faleva *et al*. 2020) and summarized in Table

3. The peak at δC/δH 71.8/4.85 ppm was assigned to aryl ether (β-O-4). The peak at δC/δH 55.6/3.72 ppm was assigned to the methoxyl group. The peaks at δC/δH 110.9/6.95 ppm, δC/δH 114.6/6.70 ppm, and δC/δH 119.1/6.78 ppm were assigned to G_2, G_5 and G_6, respectively (Mansfield *et al*. 2012; Lin *et al*. 2021; Su *et al*. 2021). The peak at δC/δH 103.8/6.68 ppm was assigned to $S_{2,6}$.

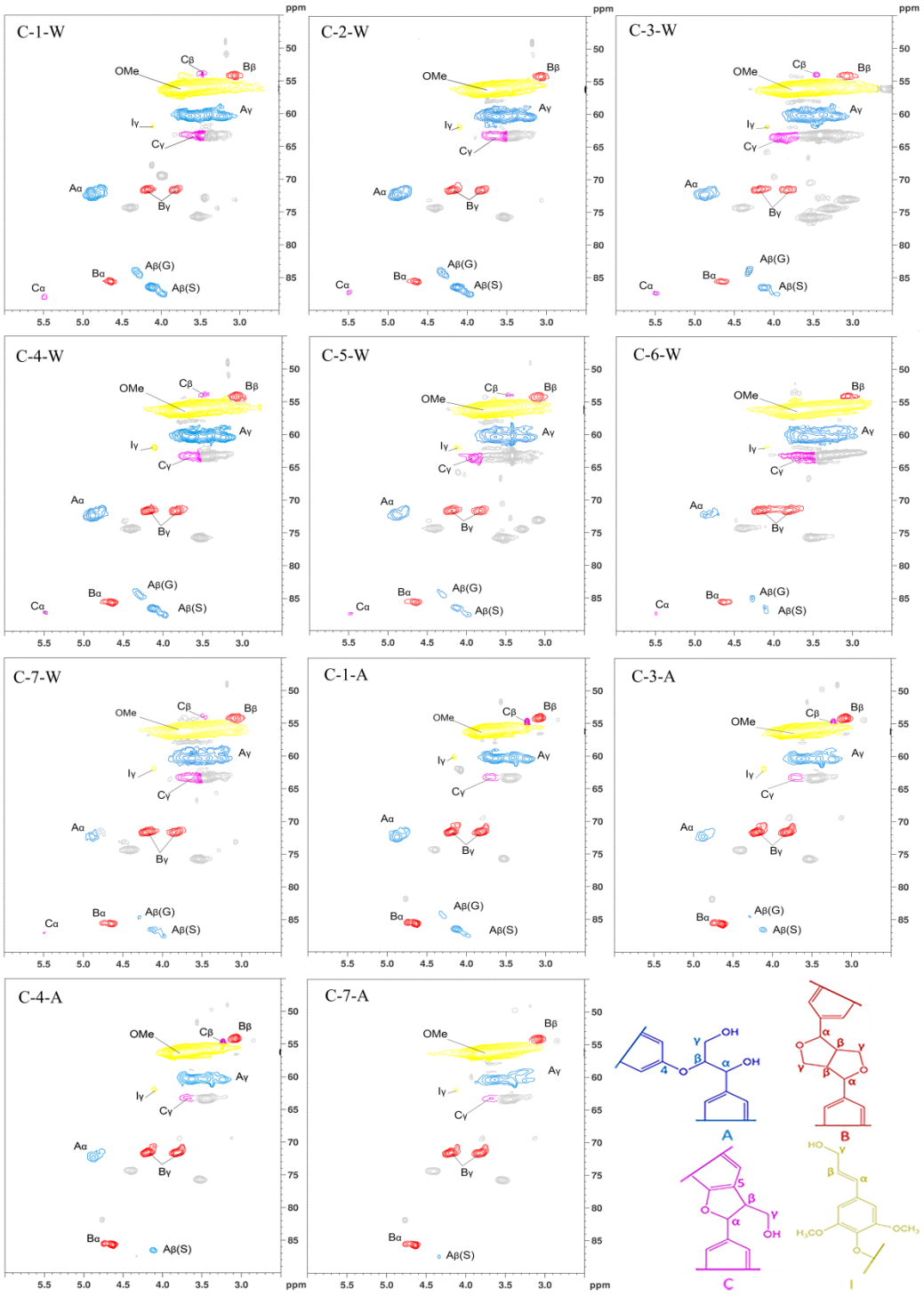

Fig. 1. 2D HSQC NMR spectra of the oxidized aliphatic region of C-X-Ws and C-X-As. The substructures of lignin were identified by 2D HSQC NMR: (A) aryl ether (β-O-4), (B) resinol (β-β); C, phenylcoumaran (β-5), (I) p-hydroxycinnamyl alcohol end groups

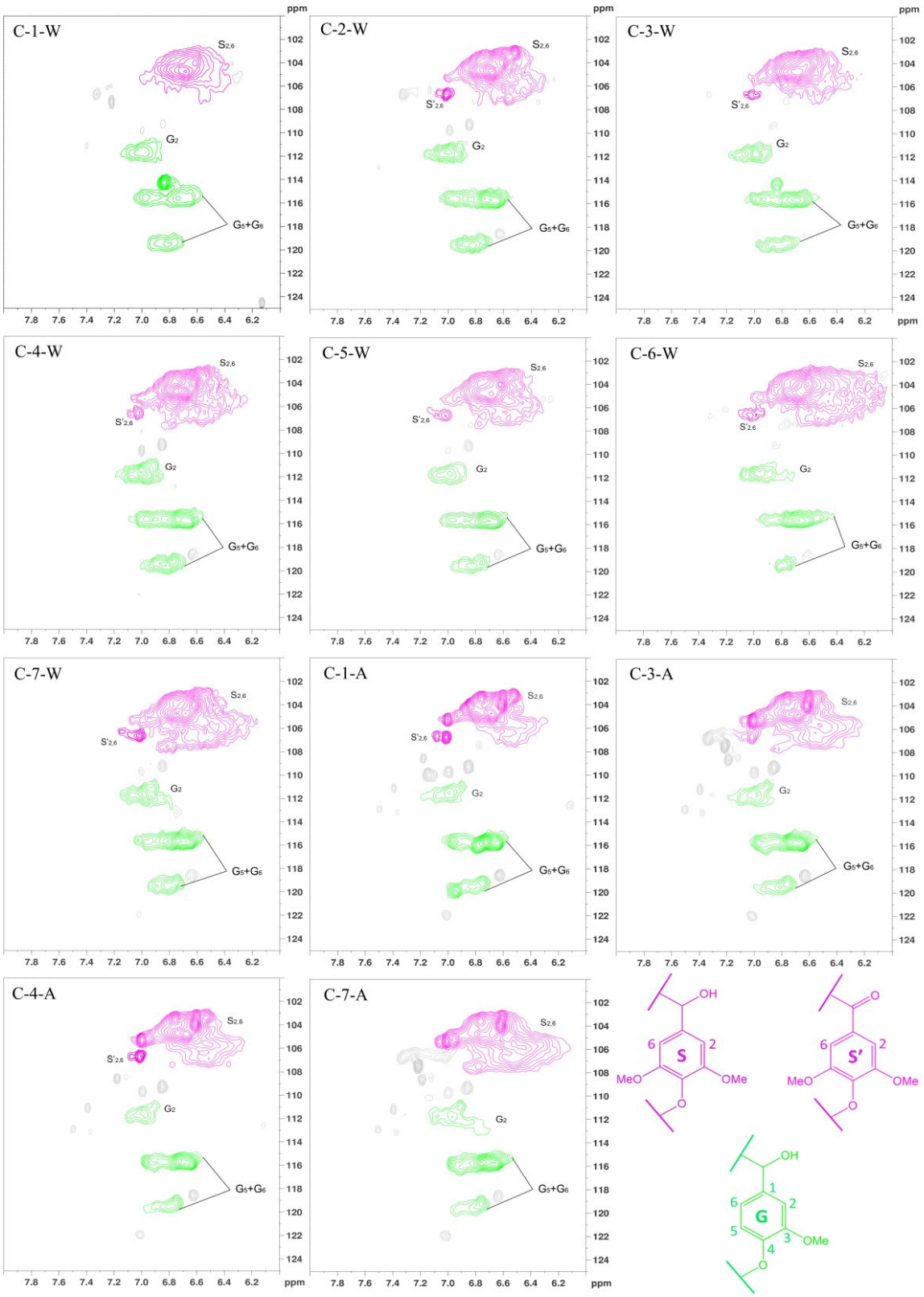

Fig. 2. 2D HSQC NMR of aromatic region of C-X-Ws and C-X-As. Lignin composing units were identified by 2D HSQC NMR: (G) guaiacyl units, (S) syringyl units, (S′) Cα-oxidized syringyl units.

Table 3. The Assignments of the Main Interunit Linkages of Lignin Preparations

Label	δ_C/δ_H	Assignment
C_β	53.1/3.46	C_β−H_β in phenylcoumaran substructures (C)
B_β	53.5/3.06	C_β−H_β in β-β′ (resinol) substructures (B)
OMe	55.6/3.72	C−H in methoxyls (−OCH_3)
A_γ	59.8/3.70	C_γ−H_γ in β-O-4′ substructures (A)
C_γ	62.6/3.76	C_γ−H_γ in phenylcoumaran substructures (C)
I_γ	61.3/4.09	C_γ−H_γ in cinnamyl alcohol end-groups (I)
B_γ	71.2/3.84-4.18	C_γ−H_γ in β-β′ resinol substructures (B)
A_α	71.8/4.85	C_α−H_α in β-O-4′ linked to a S unit (A)
B_α	84.8/4.64	C_α−H_α in β-β′ resinol substructures (B)
C_α	86.8/5.45	C_α−H_α in phenylcoumaran substructures (C)
$A_{\beta(G)}$	83.8/4.27	C_β−H_β in β-O-4′ linked to G/H unit (A)
$A_{\beta(S)}$	85.8/4.10	C_β−H_β in β-O-4′ linked to a S unit (A)
$S_{2,6}$	103.8/6.68	$C_{2,6}$−$H_{2,6}$ in syringyl units (S)
$S'_{2,6}$	106.3/7.22	$C_{2,6}$−$H_{2,6}$ in oxidized S units (S′)
G_2	110.9/6.95	C_2−H_2 in guaiacyl units (G, Non-phenolic G)
G_5	114.6/6.70	C_5−H_5 in guaiacyl units (G)
G_6	119.1/6.78	C_6−H_6 in guaiacyl units (G)

In the oxidized aliphatic region (45-95/2.5-6.0 ppm), the characteristic signals of aryl ether (A), resinol (B), and phenylcoumaran (C) were observed in lignin samples. To elucidate the changes of the linkages in the lignin samples by the cooking process, the relative abundance of linkages between the main subunits was calculated (the results were represented by 100 aromatic ring units). Table 4 shows that the fractions had different contents of the substructures. It was confirmed that β-O-4 was the most abundant linkage in the fractions. Among these lignin samples, the content of β-O-4 linkages (6.6-14.1/100Ar) in the C-X-A lignin sample was lower than in the C-X-W (23.1-31.7/100Ar) lignin sample. The fragmentation of lignin was induced by the cleavages of β-O-4 during cooking process, which reduced the molecular weight of lignin. With the increase of cooking degree, the content of β-O-4 linkages in lignin samples decreased. For example, the content of β-O-4 reduced from C-1-W (31.7/100Ar) to C-7-W (11.8/100Ar). It has been revealed that the cleavage of aryl ether bonds (β-O-4) induced the fragmentation of lignin, the generated lignin fragments further condensed into the condensed macromolecular as well during the cooking process. As a result, the condensation increased the molecular weight and enhanced the phenolic hydroxyl content of lignin. Compared to the aryl ether bond (β-O-4), the C-C bonds (*e.g.*, β-β and β-5) were more stable during the cooking process. Thus, the content of the C-C bonds (β-β and β-5) was similar. It can be concluded that the fragmentation of lignin was mainly induced by the cleavages of β-O-4 linkages.

In the aromatic region (90-160/5.5-8.3 ppm), the S/G ratio showed a trend of increasing first and then decreasing. This is because the lignin locating outside of cell wall was mainly composed by G units, which can be dissolved quickly at the early stage of cooking, while the lignin composed by G and S units mainly distributed in S2 layer (Zhou *et al*. 2011; Tolbert *et al*. 2016). In the later stages of cooking, the S/G ratio decreased because the S units mainly forming β-O-4 were easier to be cleaved than the G units mainly forming C-C substructures. Therefore, the content of β-O-4 linkages in the lignin samples can be regulated through the cooking condition.

Table 4. Quantification of the Inter-Unit Linkages and S/G Ratios of Lignin

Sample	β-O-4[a]	β-β	β-5	S/G[b]
C-1-W	31.7	5.4	1.8	1.56
C-2-W	23.2	6.6	1.8	1.65
C-3-W	25.3	9.7	1.7	1.85
C-4-W	20.8	9.3	2.1	1.77
C-5-W	23.1	10.3	1.6	1.85
C-6-W	12.6	10.8	1.5	1.93
C-7-W	11.8	12.1	1.5	1.87
C-1-A	14.1	9.4	1.4	1.71
C-3-A	11.5	8.4	1.5	1.74
C-4-A	11.5	8.5	1.5	1.74
C-7-A	6.6	6.9	0.9	1.79

[a] Results were expressed per 100 Ar based on the quantitative 2D NMR analysis. [b] S/G ratio was calculated by the equation: S/G ratio = $0.5I(S_{2,6})/I(G_2)$.

^{31}P NMR Analysis

The hydroxyl group, which is one of the most important functional groups of lignin, is the main active site for chemical modification of lignin (He *et al*. 2009; Bian *et al*. 2010; Huang *et al*. 2011). The quantification of the hydroxyl group in lignin samples by ^{31}P NMR is summarized in Table 5. The total phenolic hydroxyl content was correlated to the cooking degree. With the increase of cooking degree, the content of total phenolic hydroxyl group increased gradually. For instance, the total phenolic hydroxyl content of C-1-W, C-2-W, C-3-W, C-4-W, C-5-W, C-6-W, and C-7-W were 1.40, 1.43, 1.51, 1.50, 1.68, 1.77, and 1.75 mmol/g, which corresponded to the cleavages of aryl ether bond (β-O-4) of lignin during the cooking process.

The cleavage of β-O-4 induced the fragmentation of lignin and enhanced the solubilization of lignin, which generated new phenolic hydroxyl groups on the lignin fragments. With the increase of cooking degree, the content of syringyl (S) phenolic hydroxyl groups in the lignin samples gradually increased, and the content of guaiacyl (G) phenolic hydroxyl groups changed little. This is because the syringyl (S) unit mainly was forming aryl ether bonds which were easier to be cleaved during the cooking process. Therefore, more phenolic hydroxyl groups of the syringyl (S) fragments were gradually exposed with the increases of the cooking degree. The M_w values of C-6-W and C-7-W were not much different from other C-X-W samples, but C-6-W and C-7-W had higher phenolic hydroxyl content and lower β-O-4 linkage content. This is due to the cleavage of β-O-4 under the severe cooking condition. The fragments coupled again to form a condensed structure during the further cooking process, which eventually exposed a large number of phenolic hydroxyl groups.

According to the analysis of 2D NMR and GPC, C-6-W and C-7-W had condensed lignin-like macromolecular structure. However, C-3-W had high molecular weight and high β-O-4 linkage content but low phenolic hydroxyl content, which was prone to be a non-condensed lignin. In addition, the carboxyl groups increased with the degree of cooking, because lignin was oxidized under high-temperature and high-alkali conditions. Therefore, the content of phenolic hydroxyl groups in the lignin also can be regulated by the cooking degree.

Table 5. Quantification of Hydroxyl Groups of Lignin Samples (mmol/g)

Sample	Aliphatic OH	Syringyl OH	Guaiacyl OH	S+G OH	Carboxylic group
C-1-W	2.06	0.82	0.58	1.40	0.59
C-2-W	2.17	0.84	0.59	1.43	0.62
C-3-W	2.34	0.90	0.61	1.51	0.69
C-4-W	2.18	0.91	0.59	1.50	0.62
C-5-W	2.12	1.09	0.59	1.68	0.64
C-6-W	2.18	1.17	0.61	1.77	0.61
C-7-W	2.05	1.20	0.55	1.75	0.61

TGA Analysis

As shown in Fig. 3(a), the weight loss of the samples occurred at 100 °C, which was mainly due to the removal of moisture and the thermal decomposition of some small organic impurities. With the increase of temperature, the weight loss of lignin increased rapidly. The maximum weight loss of lignin was observed at 350 °C, and little change was identified after 600 °C. The major weight loss of lignin in this temperature range can be explained by the thermal decomposition of lignin.

Figure 3(b) indicates that the "coke residue" of the lignin samples from C-1-W to C-7-A were 55.15%, 57.18%, 54.82%, 54.74%, 54.39%, 56.87%, 57.03%, 49.35%, 53.09%, 53.09%, and 52.68%. The coke residues of C-X-W lignin samples were higher than those of the C-X-A lignin samples. C-X-W samples with the highest residual coke yields may be more valuable than the other C-X-A samples in the production of activated carbon or carbon fiber with lignin as the carbon precursor.

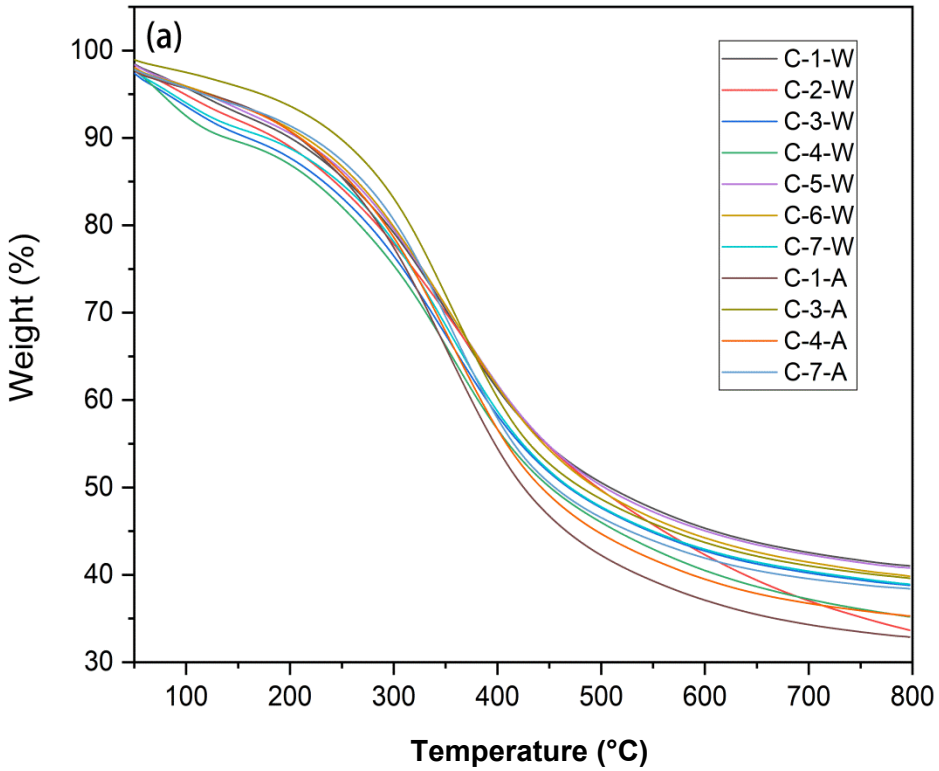

Fig. 3a. Thermal properties analysis of the isolated lignin: (a) TG curves, (b) DTG curves

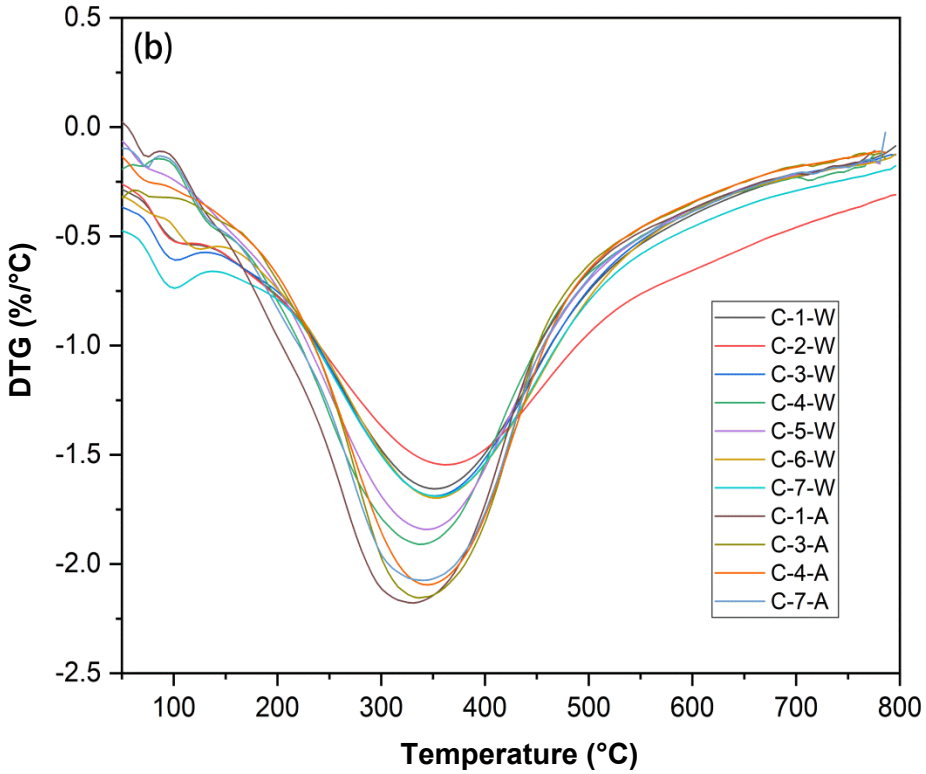

Fig. 3b. Thermal properties analysis of the isolated lignin: (a) TG curves, (b) DTG curves

The maximum decomposition temperatures (T_M) of C-1-A, C-3-A, C-4-A, and C-7-A were 325, 345, 335, and 330 °C, respectively. The maximum decomposition temperatures (T_M) from C-1-W to C-7-W were 350, 360, 355, 340, 345, 350, and 350 °C, respectively. According to previous studies (Hatakeyama and Hatakeyama 2009; Shen *et al*. 2016), the lignin with higher molecular weight possessed better thermal stability. The T_M of C-X-W was higher than the T_M of C-X-A, which confirmed that the samples with higher molecular weight had higher thermal stability.

CONCLUSIONS

1. The molecular weight, β-O-4 content and phenolic hydroxyl content of lignin can be regulated by adjusting the cooking residence time.
2. The more non-condensed C-3-W lignin sample bearing higher β-O-4 linkages and molecular weights, but lower phenolic hydroxyl content was obtained with shorter cooking time. Such a product can be applied to as a natural lignin adhesive.
3. The more condensed C-7-W lignin sample containing higher phenolic hydroxyl content was obtained with extensive cooking. This can be used as the feedstock for various chemical modifications.

ACKNOWLEDGMENTS

The authors are grateful for financial support from Science and Technology Major Project of Guangxi (2018AA16008), the Natural Science Foundation of Guangxi (2018JJA130224), the Foundation of Guangxi Key Laboratory of Clean Pulp & Papermaking and Pollution Control (ZR201805-7), and the Opening Project of National Enterprise Technology Center of Guangxi Bossco Environmental Protection Technology Co., Ltd, Nanning 530007, China.

Conflict of interest

The authors declare no conflict of interest.

REFERENCES CITED

Bian, J., Peng, F., Xu, F., Sun, R. C., and Kennedy, J. F. (2010). "Fractional isolation and structural characterization of hemicelluloses from *Caragana korshinskii*," *Carbohydr. Polym.* 80(3), 753-760. DOI: 10.1016/j.carbpol.2009.12.023

Cha, Y. L., Alam, A. M., Park, S. M., Moon, Y. H., Kim, K. S., Lee, J. E., Kwon, D. E., and Kang, Y. G. (2020). "Hydrothermal-process-based direct extraction of polydisperse lignin microspheres from black liquor and their physicochemical characterization," *Bioresource Technology* 297, article no. 122399. DOI: 10.1016/j.biortech.2019.122399

Chen, W. J., Yang, S., Zhang, Y., Wang, Y. Y., Yuan, T. Q., and Sun, R. C. (2017). "Effect of alkaline preswelling on the structure of lignins from Eucalyptus," *Sci. Rep.* 7, 10. DOI: 10.1038/srep45752

Chen, W. J., Zhao, B. C., Wang, Y. Y., Yuan, T. Q., Wang, S. F., and Sun, R. C. (2018). "Revealing the topochemistry and structural features of lignin during the growth of *Eucalyptus grandis* × *Eucalyptus urophylla*," *ACS Sustainable Chemistry & Engineering* 6(7), 9198-9207. DOI: 10.1021/acssuschemeng.8b01542

Collins, M. N., Nechifor, M., Tanasa, F., Zanoaga, M., McLoughlin, A., Strozyk, M. A., Culebras, M., and Teaca, C. A. (2019). "Valorization of lignin in polymer and composite systems for advanced engineering applications - A review," *Int. J. Biol. Macromol.* 131, 828-849. DOI: 10.1016/j.ijbiomac.2019.03.069

Culebras, M., Sanchis, M. J., Beaucamp, A., Carsí, M., Kandola, B. K., Horrocks, A. R., Panzetti, G., Birkinshaw, C., and Collins, M. N. (2018). "Understanding the thermal and dielectric response of organosolv and modified kraft lignin as a carbon fibre precursor," *Green Chemistry* 20(19), 4461-4472. DOI: 10.1039/c8gc01577e

Culebras, M., Barrett, A., Pishnamazi, M., Walker, G. M., and Collins, M. N. (2021). "Wood-derived hydrogels as a platform for drug-release systems," *Acs Sustainable Chemistry & Engineering* 9(6), 2515-2522. DOI: 10.1021/acssuschemeng.0c08022

Faleva, A. V., Kozhevnikov, A. Y., Pokryshkin, S. A., Falev, D. I., Shestakov, S. L., and Popova, J. A. (2020). "Structural characteristics of different softwood lignins according to 1D and 2D NMR spectroscopy," *Journal of Wood Chemistry and Technology* 40(3), 178-189. DOI: 10.1080/02773813.2020.1722702

Fu, K., Yue, Q., Gao, B., Sun, Y., and Zhu, L. (2013). "Preparation, characterization and application of lignin-based activated carbon from black liquor lignin by steam activation," *Chemical Engineering Journal* 228, 1074-1082. DOI:

10.1016/j.cej.2013.05.028

Gall, D. L., Ralph, J., Donohue, T. J., and Noguera, D. R. (2017). "Biochemical transformation of lignin for deriving valued commodities from lignocellulose," *Curr. Opin. Biotechnol.* 45, 120-126. DOI: 10.1016/j.copbio.2017.02.015

Gellerstedt, G., and Zhang, L. M. (2001). "Lignin fractionation and quantitative structural analysis of the lignin fractions with ^{13}C and HSQC NMR techniques," in: *Workshop on Advanced Methods for Lignocellulosics and paper Products Characterization*.

Gellerstedt, G., and Zhang, L. M. (2000). "Achieving quantitative assignment of lignin structure by combining ^{13}C and HSQC NMR techniques," in: *European Workshop on Lignocellulosics & Pulp*.

Gillet, S., Aguedo, M., Petitjean, L., Morais, A. R. C., Costa Lopes, A. M. D., Łukasik, R. M., and Anastas, P. T. (2017). "Lignin transformations for high value applications: towards targeted modifications using green chemistry," *Green Chemistry* 19(18), 4200-4233. DOI: 10.1039/c7gc01479a

Gong, W. H., Xiang, Z. Y., Ye, F. Y., and Zhao, G. H. (2016). "Composition and structure of an antioxidant acetic acid lignin isolated from shoot shell of bamboo (*Dendrocalamus latiforus*)," *Industrial Crops and Products* 91, 340-349. DOI: 10.1016/j.indcrop.2016.07.023

Hatakeyama, H., and Hatakeyama, T. (2009). "Lignin structure, properties, and applications," *Advances in Polymer Science* 232, 1-63. DOI: 10.1007/12_2009_12

He, Z. Q., Mao, J. D., Honeycutt, C. W., Ohno, T., Hunt, J. F., and Cade-Menun, B. J. (2009). "Characterization of plant-derived water extractable organic matter by multiple spectroscopic techniques," *Biology and Fertility of Soils* 45(6), 609-616. DOI: 10.1007/s00374-009-0369-8

Himmel, M. E., Ding, S. Y., Johnson, D. K., Adney, W. S., Nimlos, M. R., Brady, J. W., and Foust, T. D. (2007). "Biomass recalcitrance: Engineering plants and enzymes for biofuels production," *Science* 315(5813), 804-807. DOI: 10.1126/science.1137016

Holtman, K. M., Chang, H. M., and Kadla, J. F. (2007). "An NMR comparison of the whole lignin from milled wood, MWL, and REL dissolved by the DMSO/NMI procedure," *Journal of Wood Chemistry and Technology* 27(3-4), 179-200. DOI: 10.1080/02773810701700828

Huang, F., Singh, P. M., and Ragauskas, A. J. (2011). "Characterization of milled wood lignin (MWL) in loblolly pine stem wood, residue, and bark," *J. Agric. Food Chem.* 59(24), 12910-12916. DOI: 10.1021/jf202701b

Jardim, J. M., Hart, P. W., Lucia, L., and Jameel, H. (2020). "Insights into the potential of hardwood kraft lignin to be a green platform material for emergence of the biorefinery," *Polymers* 12(8). DOI: 10.3390/polym12081795

Kim, H., and Ralph, J. (2010). "Solution-state 2D NMR of ball-milled plant cell wall gels in DMSO-d6/pyridine-d5," *Organic & Biomolecular Chemistry* 8(3), 576-591. DOI: 10.1039/b916070a

Lin, S. Y., and Dence, C. W. (1992). *Methods in Lignin Chemistry*, Springer, New York. DOI: 10.1007/978-3-642-74065-7

Lin, M. S., Yang, L. J., Zhang, H., Xia, Y., He, Y., Lan, W., Ren, J. L., Yue, F. X., and Lu, F. C. (2021). "Revealing the structure-activity relationship between lignin and anti-UV radiation," *Industrial Crops and Products*. 174. DOI: 10.1016/j.indcrop.2021.114212

Lora, J. H., and Glasser, W. G. (2002). "Recent industrial applications of lignin: A sustainable alternative to nonrenewable materials," *Journal of Polymers and the*

Environment 10(1-2), 39-48. DOI: 10.1023/A:1021070006895

Lourenco, A., Rencoret, J., Chemetova, C., Gominho, J., Gutierrez, A., Del Rio, J. C., and Pereira, H. (2016). "Lignin composition and structure differs between xylem, phloem and phellem in *Quercus suber* L," *Front. Plant Sci*. 7, 1612. DOI: 10.3389/fpls.2016.01612

Magdeldin, M., and Jarvinen, M. (2020). "Supercritical water gasification of Kraft black liquor: Process design, analysis, pulp mill integration and economic evaluation," *Applied Energy* 262, 19. DOI: 10.1016/j.apenergy.2020.114558

Mansfield, S. D., Kim, H., Lu, F. C., and Ralph, J. (2012). "Whole plant cell wall characterization using solution-state 2D NMR," *Nature Protocols*. 7(9), 1579-1589. DOI: 10.1038/nprot.2012.064

Martínez, A. T., Rencoret, J., Marques, G., Gutiérrez, A., Ibarra, D., Jiménez-Barbero, J., and Del Rio, J. C. (2008). "Monolignol acylation and lignin structure in some nonwoody plants: A 2D NMR study," *Phytochemistry* 69(16), 2831-2843. DOI: 10.1016/j.phytochem.2008.09.005

Meng, X. Z., Crestini, C., Ben, H. X., Hao, N. J., Pu, Y. Q., Ragauskas, A. J., and Argyropoulos, D. S. (2019). "Determination of hydroxyl groups in biorefinery resources via quantitative 31P NMR spectroscopy," *Nature Protocols* 14(9), 2627-2647. DOI: 10.1038/s41596-019-0191-1

Menon, V., and Rao, M. (2012). "Trends in bioconversion of lignocellulose: Biofuels, platform chemicals & biorefinery concept," *Progress in Energy and Combudtion Science* 38(4), 522-550. DOI: 10.1016/j.pecs.2012.02.002

Milotskyi, R., Szabo, L., Takahashi, K., and Bliard, C. (2019). "Chemical modification of plasticized lignins using reactive extrusion," *Frontiers in Chemistry* 7, 633. DOI: 10.3389/fchem.2019.00633

Narapakdeesakul, D., Sridach, W., and Wittaya, T. (2013). "Recovery, characteristics and potential use as linerboard coatings material of lignin from oil palm empty fruit bunches' black liquor," *Industrial Crops and Products* 50, 8-14. DOI: 10.1016/j.indcrop.2013.07.011

Ragauskas, A. J., Beckham, G. T., Biddy, M. J., Chandra, R., Chen, F., Davis, M. F., Davison, B. H., Dixon, R. A., Gilna, P., Keller, M., *et al*. (2014). "Lignin valorization: Improving lignin processing in the biorefinery," *Science* 344(6185), 1246843. DOI: 10.1126/science.1246843

Rencoret, J., Gutiérrez, A., Nieto, L., Jiménez-Barbero, J., Faulds, C. B., Kim, H., Ralph, J., Martínez, A. T., and Del Rio, J. C. (2011). "Lignin composition and structure in young versus adult *Eucalyptus globulus* plants," *Plant Physiology* 155(2), 667-682. DOI: 10.1104/pp.110.167254

Rencoret, J., Marques, G., Gutiérrez, A., Nieto, L., Jiménez-Barbero, J., Martinez, A. T., and Del Rio, J. C. (2009). "Isolation and structural characterization of the milled-wood lignin from *Paulownia fortunei* wood," *Industrial Crops and Products* 30(1), 137-143. DOI: 10.1016/j.indcrop.2009.03.004

Rencoret, J., Marques, G., Gutiérrez, A., Nieto, L., Santos, J. I., Barbero. J. J., Martínez. A. T., and Río. J. C. D. (2009). "HSQC-NMR analysis of lignin in woody (*Eucalyptus globulus* and *Picea abies*) and non-woody (*Agave sisalana*) ball-milled plant materials at the gel state," *Holzforschung*. 63, 691-698. DOI: 10.1515/HF.2009.070

Shen, X. J., Wang, B., Huang, P. L., Wen, J. L., and Sun, R. C. (2016). "Understanding the structural changes and depolymerization of *Eucalyptus* lignin under mild conditions in aqueous $AlCl_3$," *RSC Adv.* 6(51), 45315-45325. DOI:

10.1039/c6ra08945c
Su, S. H., Wang, S. Z., and Song, G. Y. (2021). "Disassembling catechyl and guaiacyl/syringyl lignins coexisting in Euphorbiaceae seed coats," *Green Chemistry*. 23(18), 7235-7242. DOI: 10.1039/d1gc02131a
Tolbert, A., Akinosho, H., Khunsupat, R., Naskar, A. K., and Ragauskas, A. J. (2014). "Characterization and analysis of the molecular weight of lignin for biorefining studies," *Biofuels Bioproducts & Biorefining-Biofpr* 8(6), 836-856. DOI: 10.1002/bbb.1500
Tolbert, A. K., Ma, T., Kalluri, U. C., and Ragauskas, A. J. (2016). "Determining the syringyl/guaiacyl lignin ratio in the vessel and fiber cell walls of transgenic populus plants," *Energy & Fuels*. 30(7), 5716-5720. DOI: 10.1021/acs.energyfuels.6b00560
Wang, H. M., Wang, B., Wen, J. L., Yuan, T. Q., and Sun, R. C. (2017). "Structural characteristics of lignin macromolecules from different *Eucalyptus* species," *ACS Sustainable Chemistry & Engineering* 5(12), 11618-11627. DOI: 10.1021/acssuschemeng.7b02970
Wen, J. L., Sun, S. L., Yuan, T. Q., and Sun, R. C. (2015). "Structural elucidation of whole lignin from Eucalyptus based on preswelling and enzymatic hydrolysis," *Green Chemistry* 17(3), 1589-1596. DOI: 10.1039/c4gc01889c
Wen, J. L., Xue, B. L., Xu, F., Sun, R. C., and Pinkert, A. (2013). "Unmasking the structural features and property of lignin from bamboo," *Industrial Crops and Products* 42, 332-343. DOI: 10.1016/j.indcrop.2012.05.041
Xiao, M. Z., Chen, W. J., Hong, S., Pang, B., Cao, X. F., Wang, Y. Y., Yuan, T. Q., and Sun, R. C. (2019). "Structural characterization of lignin in heartwood, sapwood, and bark of eucalyptus," *Int J Biol Macromol* 138, 519-527. DOI: 10.1016/j.ijbiomac.2019.07.137
Xiong, W. L., Qiu, X. Q, Yang, D. J., Zhong, R. S., Qian, Y., Li, Y. Y., and Wang, H. (2017). "A simple one-pot method to prepare UV-absorbent lignin/silica hybrids based on alkali lignin from pulping black liquor and sodium metasilicate," *Chemical Engineering Journal* 326, 803-810. DOI: 10.1016/j.cej.2017.05.041
Zhang, L. M., and Gellerstedt, G. (2001). "NMR observation of a new lignin structure, a spiro-dienone," *Chemical Communications* 24, 2744-2745 DOI: 10.1039/b108285j
Zhang, L. M., and Gellerstedt, G. (2011). "Quantitative 2D HSQC NMR determination of polymer structures by selecting suitable internal standard references," *Magnetic Resonance in Chemistry* 45(1), 37-45. DOI: 10.1002/mrc.1914
Zhou, C. Z., Li, Q. Z., Chiang, V. L., Lucia, L. A., and Griffis, D. P. (2011). "Chemical and spatial differentiation of syringyl and guaiacyl lignins in poplar wood via time-of-flight secondary ion mass spectrometry," *Analytical Chemistry*. 83(18), 7020-7026. DOI: 10.1021/ac200903y

Article submitted: March 22, 2022; Peer review completed: April 8, 2022; Revised version received and accepted: May 15, 2022; Published: May 23, 2022.
DOI: 10.15376/biores.17.3.4226-4240